© 1999 The Chemical Society of Japan

Structural Genealogy of BEDT-TTF-Based Organic Conductors III. Twisted Molecules: δ and α' Phases

Takehiko Mori

Department of Organic and Polymeric Materials, Tokyo Institute of Technology, O-okayama, Tokyo 152-8552

(Received February 4, 1999)

δ-phase (β-PF_6 type) BEDT-TTF (bis(ethylenedithio)tetrathiafulvalene)-based organic conductors are characterized by the twisted overlap mode in the stack. Since the twisted mode has large intermolecular orbital overlap, the δ-phase is regarded as a twisted dimer structure. This type of overlap is, however, insensitive to small changes of the structure. On the contrary, an oblique interaction alters the warping of the open Fermi surface, to control the metal-insulator transition temperature, T_{MI}. Through the change of this oblique interaction, T_{MI} is scaled by the axis ratio for a family of salts with the same stacking pattern. As a general summary of BEDT-TTF salts, an empirical rule is proposed to predict, from the number of crystallographically independent molecules, whether an insulating state of BEDT-TTF salts will be paramagnetic or nonmagnetic. This rule is based on hypothetical pair formation of spins located on each dimer, and universally applies to all BEDT-TTF salts. This rule is extended to metallic salts, and among the potentially nonmagnetic salts, a dimerized dimer structure is the necessary condition of superconductivity. The potentially paramagnetic superconductors have strongly dimerized structures like β and $\varkappa$ phases. From this we can make a reasonable prediction as to superconducting phases.

In Part I of the present series,[1] from the viewpoint of quantum chemical calculation, we have examined how the overlap integral between HOMO's of two parallel BEDT-TTF (or ET for short) molecules changes depending on the relative geometry of the two molecules. We have investigated the dependence of overlap integrals on two geometry parameters: (1) the angle ϕ between the molecular plane and the intermolecular vector, and (2) the displacement D along the molecular long axis. In the actual crystals, two kinds of geometry, ring-over-bond (RB) mode (ϕ = 90° and D = 1.6 Å) and ring-over-atom (RA) mode (ϕ = 60° and D = 0.0 Å), appear most frequently, and are regarded as essential building blocks. We have proposed a genealogy of ET salts in which several different ways to pile up these elements lead to various structures which are conventionally designated as β, β', β'', θ, α, and α''-phases.

There is another type of frequently observed molecular arrangement: Twisted overlap (Fig. 1), where the molecular long axes are not parallel any more, but the molecular planes are parallel to each other.[2] A classical example which contains this structure is β-$(ET)_2PF_6$ and β-$(ET)_2AsF_6$ (Fig. 2). Although these salts are called β, this name is only based on historical origin (see Appendix in Part I), and this salt has no structural relation to the β-phase. There are a considerable number of salts classified in this family (Table 1). Since this family is sometimes called δ-phase after δ-$(ET)_2AuI_2$ and δ-$(ET)_2AuBr_2$, in this paper we shall designate this family as δ-phase. So-called α'-phase has a related structure and will be discussed as well.

A comparatively small number of studies have been undertaken for this family, because of the relatively poor conducting properties; many members of this family are insulating

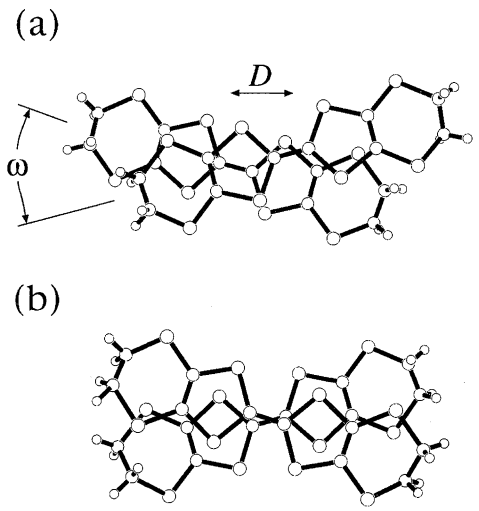

Fig. 1. Twisted overlap modes in (a) β-$(ET)_2AsF_6$ (D = 2.6 Å and ω = 30.8°) and (b) δ-$(ET)_2AuBr_2$ (D = 0.3 Å and ω = 34.1°). These overlaps correspond to the a1 interaction in Fig. 2. The parameters D and ω define the geometry of this overlap mode; D is the displacement along the molecular long axes, and ω is the angle between the molecular long axes.

even at room temperature, or undergo metal-insulator transitions at fairly high temperatures. No superconducting salt has been found among this family. Nevertheless this family is as important as other phases from the structural point of view, because the twisted overlap is universally found in ET conductors. The twisted overlap mode is regarded as the third overlap pattern of ET, together with the RB and RA modes, which avoids steric repulsion when ET molecules

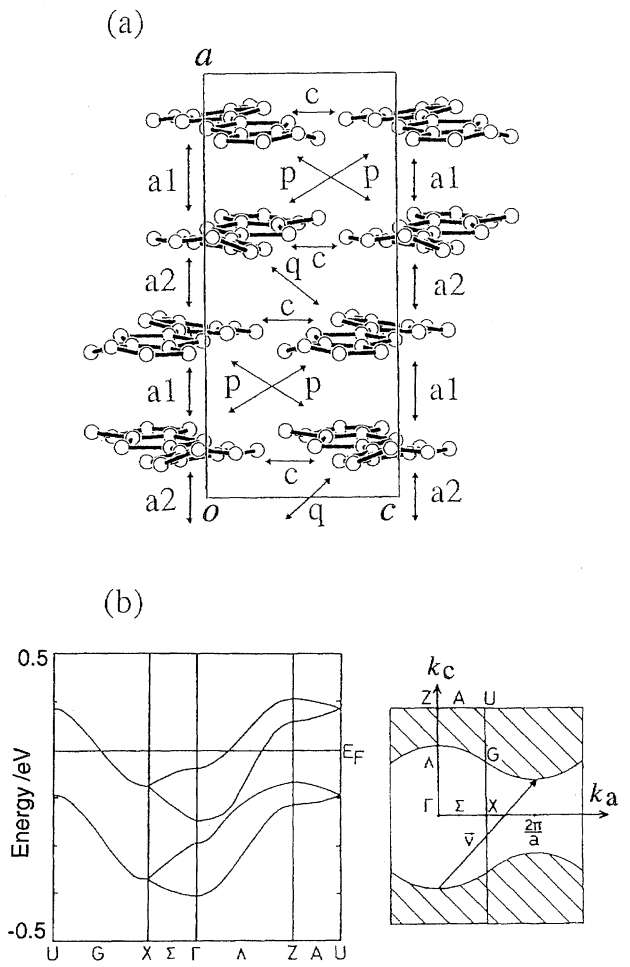

Fig. 2. (a) Structure of the donor sheet in β-$(ET)_2AsF_6$, viewed approximately along the molecular long axis. (b) Energy band structure and Fermi surface of β-$(ET)_2AsF_6$.[5] The Fermi surface is depicted in the extended zone scheme, where the k_a direction is doubled on the basis of the degeneracy on the X–G–U zone boundary, which originates in the a glide plane.

make stacks. In the present paper, we shall examine how the overlap integral changes as a function of the geometry of the twisted molecules, as we have done for two parallel molecules in Part I.

In Part II of this series we have discussed the "universal phase diagram" of θ- and $\varkappa$-phases.[31] In these phases, the metal-insulator transition temperatures T_{MI} are scaled by the axis ratio c/a, namely the ratio of lattice constants within the conducting sheet. This logic is based on the idea that the overlap integral between nonparallel ET molecules is a sensitive function of the dihedral angle between the ET molecules. The axis ratio alters the dihedral angle so as to modify the overlap integral, which in turn regulates the bandwidth W. In the present paper, we will show that T_{MI} of the δ-phase is also scaled by the axis ratio. Here the "key" interaction which regulates T_{MI} is not the twisted overlap itself, but an oblique interaction designated as q in Fig. 2. This interaction modifies the warping of the Fermi surface, to change T_{MI}. In the course of this study, we have found different types of stacking patterns of the δ-phases. Though these patterns have not been recognized sufficiently so far, the difference has to be taken into account for discussing the physical properties.

To conclude this series, in the latter half of this paper, we will discuss some empirical rules which are applied to all ET salts. When an ET conductor undergoes a metal-insulator transition, some salt becomes nonmagnetic accompanied by drop of the magnetic susceptibility in an activated manner, like the Peierls transition. However, other salts remain paramagnetic, where the magnetic susceptibility follows the two-dimensional (or one-dimensional) Heisenberg model continuously from the metallic to the insulating regions. This distinction is predictable from the symmetry of the crystal. When the spins are hypothetically located on dimers, if the spins make pairs from the crystal symmetry, the system becomes nonmagnetic; otherwise it becomes paramagnetic. To decide this distinction easily, the concept of "symmetry number" is introduced. The symmetry number η is a product of the number of ET molecules in a unit cell and the number of crystallographically independent molecules. In a quarter-filled case, the salts with $\eta \leq 4$ have a paramagnetic insulating state, whereas those with $\eta > 4$ are nonmagnetic.

We can define the symmetry number even for the salts which do not have any insulating state. As an extreme case, we can divide ET-based superconductors into "potentially paramagnetic" and "potentially nonmagnetic" groups. The potentially nonmagnetic superconductors have a common structural characteristic; all salts that show superconductivity have a "dimerized dimer" structure. In the potentially paramagnetic superconductors, the two-dimensional large connected Fermi surface as well as the dimer structure are necessary conditions for showing superconductivity. From these considerations, we can make a fairly good prediction as to superconductivity.

Twisted Molecules

Crystal and Energy Band Structures of δ-Phase. The donor sheet structure of β-$(ET)_2AsF_6$ is depicted in Fig. 2(a).[5,6,32,33] In the following discussion, crystal axes are transformed so as to coincide with those of β-$(ET)_2PF_6$. Although it has been previously reported that β-$(ET)_2AsF_6$ (monoclinic) belongs to a different crystal system from β-$(ET)_2PF_6$ (orthorhombic),[5] the recent re-examination of the crystal structure has shown that β-$(ET)_2AsF_6$ is exactly isostructural to β-$(ET)_2PF_6$.[6]

In the stacking (crystallographic a) direction, four ET molecules make the repeating unit, but owing to the crystal symmetry, the stack comprises two overlap modes a1 and a2. Here, only one ET molecule is crystallographically independent. In the interaction a1, as shown in Fig. 1(a), the molecular long axes are not parallel. We shall call this kind of overlap mode twisted interaction. The molecules interacting through the a1 interaction are connected by a two-fold axis running along the crystallographic c axis (Fig. 3(a)). As a consequence, the molecular planes are parallel to each other. The interplanar distance is 3.48 Å The molecular long

Table 1. Lattice Parameters of δ-Phase (β-PF_6 Type) ET Salts[a)]

Compounds	a/Å	b/Å	c/Å	c/a	T_{MI}	Ref.
δ-Phases with crystallographically independent one molecule in a sheet						
$(ET)_2Au(CN)_2Cl_2$	15.284	17.726	6.690	0.4377	250 K	3
$(ET)_2CF_3SO_3$	15.018	33.050	6.649	0.4427	306 K	4
β-$(ET)_2PF_6$	14.960	32.643	6.664	0.4455	297 K	2
β-$(ET)_2AsF_6$	15.025	33.072	6.695	0.4456	264 K	5,6,32
$(ET)_2C(CN)_3$	14.979	16.395	6.700	0.4473	180 K	7,8
β-$(ET)_2SbF_6$	14.93	33.56	6.70	0.4488	273 K	5
δ-$(ET)_2Ni(CN)_4(H_2O)_4$	15.084	17.466	6.771	0.4489	180 K	9
$(ET)_2Br(H_2O)_3$	14.993	32.779	6.734	0.4491	150 K	10
δ-$(ET)_2Pt(CN)_4(H_2O)_4$	15.030	17.403	6.767	0.4502	150 K	9
$(ET)_2Cl(H_2O)_3$	14.854	32.575	6.709	0.4517	120 K	11
$(ET)_2Cl(H_2O)_2$	14.38	17.20	6.684	0.4648	20 K	12
δ-$(ET)_2AuBr_2$	14.837	32.624	6.798	0.4582	320 K	13
δ-$(ET)_2AuI_2$	14.914	33.586	6.849	0.4592	Insulator	14,15
δ'-Phases with crystallographically independent two molecules in a sheet						
$(ET)_2GaCl_4$	16.580	31.911	6.645	0.4008	I	16
$(ET)_2FeCl_4$	15.025	17.805	6.626	0.4410	I (10^{-2} S cm^{-1})	18
$(ET)_2BrC_2H_4(OH)_2$	14.950	33.692	6.621	0.4429	196 K	19
$(ET)_2InI_4$	14.961	19.440	6.715	0.4488	I	20
$(ET)_2GaI_4$	14.950	19.216	6.719	0.4494	I	20
$(ET)_4Hg_2Br_6(TCE)$[a)]	29.418(/2)	19.344	13.401(/2)	0.4555	?	17
$(ET)_2FeCl_4$	16.620	31.940	6.651	0.4002	230 K	21
α'-Phases[b)]						
$(ET)_2PF_6(C_4H_8O_2)$	8.293	33.020	6.703	0.4041	?	22
$(ET)_2ClO_4$(Dioxane)	8.242	32.998	6.677	0.4051	I (10^{-2} S cm^{-1})	23
$(ET)_2CuCl_2$	7.940	30.554	6.671	0.4201	I (10^{-2} S cm^{-1})	24
$(ET)_2C_4(CN)_6$	7.958	34.212	6.725	0.4225	I (0.017 S cm^{-1})	8
α'-$(ET)_2Ag(CN)_2$	7.956	30.738	6.732	0.4231	Insulator	25
α'-$(ET)_2Au(CN)_2$	7.932	31.018	6.735	0.4245	Insulator	25
$(ET)_2(CH_3C_6H_4SO_3)$	7.785	34.402	6.697	0.4301	Insulator	4
α'-$(ET)_2AuBr_2$	7.799	31.756	6.723	0.4310	Insulator	25
$(ET)_2N(CN)_2$	14.744/2	32.151	6.676	0.4528	?	26
$(ET)_2C_5(CN)_5(TCE)_x$	14.657/2	41.05	6.774	0.4621	I (0.4 S cm^{-1})	27
Other modifications[b)]						
$(ET)_2$(MeO-TCA)[c)]	7.856	39.765	13.419/2	0.4270	I (10^{-3} S cm^{-1})	28
γ'-$(ET)_2AuI_2$	7.738	34.16	12.833/2	0.4146	Insulator	29
$(ET)_3(HgCl_3)_2$	11.24/(3/4)	36.36	6.645	0.4434	I (10^{-2} S cm^{-1})	30

a) Lattice constants are transformed so as to coincide with other crystals. b) The values of c/a are modified so as to correspond to the ordinary δ-phase, namely the a axes are converted to the values for four molecules. c) MeO–TCA$^-$: 1,1,3,3-tetracyano-2-methoxy-2-propen-1-ide.

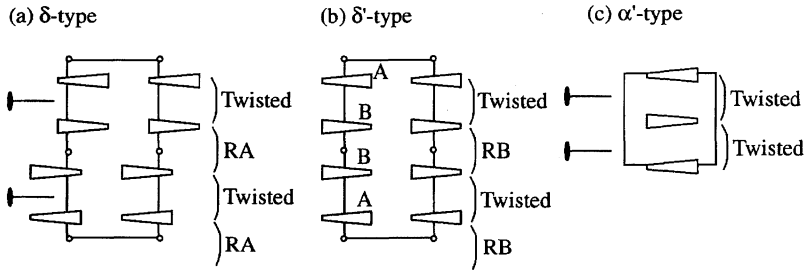

Fig. 3. Stacking patterns of (a) δ-phase, (b) δ'-phase, and (c) α'-phase.

axes make an angle ω = 30.8°, and the molecules are slid by D = 2.6 Å along the molecular long axis; the definitions of ω and D are indicated in Fig. 1(a).

Another stacking mode a2 is a typical RA overlap (ϕ = 62°

and D = 0.1 Å see Table 2). Because these molecules are related by an inversion center, their molecular planes and molecular long axes are parallel to each other. Among the transverse interactions, the interactions c and q are parallel interactions, whereas the interaction p is a kind of twisted interaction.

Intermolecular overlap integrals of HOMO's and geometry parameters are listed in Table 2.[33] The semiempirical parameters used in the present calculations are the same as those in Parts I and II, and are even the same as those in the report in 1985.[33] Since the twisted interaction a1 = 13.1×10^{-3} for β-$(ET)_2AsF_6$ is much larger than the RA interaction a2 = -2.8×10^{-3}, there is considerable dimerization in the stacking direction. We shall call this structure a "twisted dimer" structure. However, the transverse and oblique interactions, c, p, and q are significantly large; in particular the interaction q is larger than the a1 interaction. In the interactions c and q, the ϕ values are 4° and 37° respectively. Because these ϕ values are close to maxima of overlap in parallel molecules (Part I), these interactions afford large overlaps. In this respect the twisted dimer structure in the present compound is not a simple dimer structure.

Table 2. Overlap Integrals ($\times10^{-3}$) and Geometry Parameters[a] in $(ET)_2Br(H_2O)_3$, $(ET)_2AsF_6$, $(ET)_2Au(CN)_2Cl_2$, and δ-$(ET)_2AuBr_2$

Interaction	Overlap $\times10^{-3}$	$X(D)$/Å	Y/Å	Z/Å	ϕ/°	ω/°
$(ET)_2Br(H_2O)_3$						
a1	9.2	2.2	(0.8)	(3.6)	(77)	29.5
a2	−6.9	0.5	2.0	3.7	62	
c	8.8	1.7	6.5	0.4	4	
p	2.3	3.9	(5.6)	(4.0)	(35)	
q	17.2	1.2	4.5	3.2	35	
$(ET)_2AsF_6$						
a1	13.1	2.6	(0.9)	(3.5)	(75)	30.8
a2	−2.8	0.1	2.0	3.8	62	
c	10.3	1.7	6.5	0.4	4	
p	3.6	4.3	(5.6)	(3.9)	(35)	
q	16.5	1.6	4.5	3.4	37	
$(ET)_2Au(CN)_2Cl_2$						
a1	8.26	2.7	(1.0)	(3.6)	(74)	30.9
a2	−0.5	0.1	1.7	3.8	65	
c	7.4	1.8	6.4	0.5	4	
p	2.0	4.5	(5.4)	(4.0)	(36)	
q	13.8	1.7	4.7	3.3	35	
δ-$(ET)_2AuBr_2$						
a1	9.2	0.3	(0.1)	(3.8)	(89)	34.1
a2	−5.7	0.1	1.9	3.6	62	
c	8.7	2.0	6.5	0.3	2	
p	1.8	2.3	(6.6)	(3.6)	(29)	
q	8.9	1.9	4.6	3.4	36	

a) Geometry parameters have been defined in Fig. 1 in Part I. The parameters, Y, Z, and ϕ are not defined for the twisted interactions a1 and p, but are estimated from the molecular coordinates of one molecule and the center of another molecule. These values, however, indicate that the geometry of these overlap is almost the same for the δ-phase salts.

The energy band structure of this compound has already been extensively discussed in Ref. 33. The energy band is represented by the following analytical form.

$$E(k) = 2t_c \cos k_c c \pm (\Gamma \pm \Delta)^{1/2}$$
$$\Gamma = (t_{a1} + 2t_p \cos k_c c)^2 + t_{a2}^2 + t_q^2 + 2t_{a2}t_q \cos k_c c$$
$$\Delta = 2(t_{a1} + 2t_p \cos k_c c)(t_{a2}^2 + t_q^2 + 2t_{a2}t_q \cos k_c c)^{1/2} \cos(k_a a/2) \quad (1)$$

The energy band structure is depicted in Fig. 2(b). The above Γ term generates the separation of the upper two and the lower two energy bands. This is a consequence of the twisted dimer structure. The principal dispersion along the c axis comes from the first $2t_c \cos k_c c$ term. Though the c interaction is smaller than a1 and q, this c interaction determines the main dispersion which makes the Fermi surface open with respect to the transverse (c) axis. This band structure is in agreement with the observation of two-fold satellite reflections along c.[2,6] If the interaction along c is regarded as a simple uniform interaction, $2k_F$ in a quarter-filled band corresponds to four-fold modulation, and the two-fold satellite corresponds to $4k_F$ lattice distortion. Figure 2, however, indicates that in the twisted dimer structure $2k_F$ is two-fold modulation. This agrees with the observation of activated magnetic susceptibility below T_{MI}.[6,34] The Δ term in the above equation, which is proportional to $\cos(k_a a/2)$, decides the warping of the Fermi surface along a.

Twisted Overlap. In order to investigate why the twisted overlap leads to the significantly large a1 interaction, we shall examine how the overlap integral of the twisted molecules changes as a function of the geometry, D and ω. As a model calculation, the overlap integral is calculated as a function of both D and ω (Fig. 4), where the interplanar spacing is kept at 3.5 Å.

The most striking feature is that the overlap is positive everywhere, and does not cross zero. This is reasonable because HOMO of ET is a π-orbital in which all sulfur pπ-orbitals have positive signs. When we follow the curve at D = 0.0 Å along the rear wall, the overlap attains two

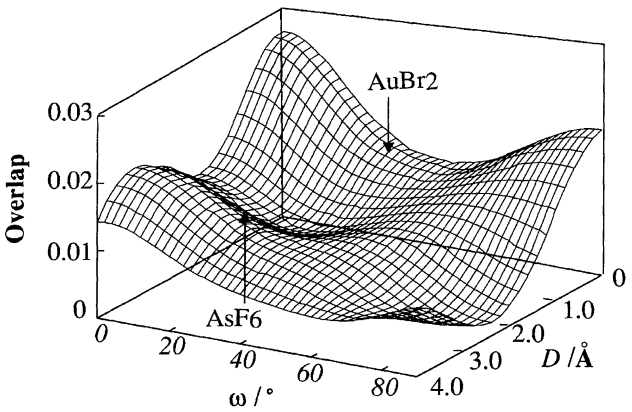

Fig. 4. Overlap integrals between HOMO's of ET as a function of D and ω. The arrow indicates the a1 interactions in β-$(ET)_2AsF_6$ and δ-$(ET)_2AuBr_2$. Although the face-to-face overlap of π-orbitals with the same orientation of the sign gives negative overlap, the absolute values are plotted.

maxima at $\omega = 0°$ and 90°. The former corresponds to an entirely eclipsed overlap. In the latter, the two molecules are perpendicular to each other, and a sulfur atom of the inner 1,3-dithiole ring comes approximately on the top of another sulfur atom; this is another kind of eclipsed mode. From the symmetry, Fig. 3 is symmetrical with respect to $\omega = 90°$. When D increases, this peak shifts to lower ω, and disappears above $D = 2.8$ Å

The curve on the left wall represents the D dependence at $\omega = 0°$; this is overlap in parallel molecules. The overlap attains a maximum at $D = 0.0$ Å a minimum at $D = 1.6$ Å and again a maximum at $D = 3.2$ Å This is the same as the modulation already observed in parallel molecules (Fig. 2(b) in Part I). The origin is eclipsed overlaps of the 1,3-dithiole rings at $D = 0.0$ and 3.2 Å.

When we increase ω, two ridges which start at $D = 0.0$ and 3.2 Å extend to the right, though the overlap decreases gradually. The position of the actual a1 interactions are close to these ridges. The a1 interaction of β-$(ET)_2AsF_6$ lies at $D = 2.6$ Å and $\omega = 30.8°$; this is near the second ridge. As shown in Fig. 1(a), this geometry is regarded as a staggered overlap, though at $\omega = 0.0$ Å the same ridge starts from an eclipsed overlap mode. The actual overlap at $D = 2.6$ Å and $\omega = 30.8°$ realizes not only a large overlap of orbitals but also a preferable overlap that avoids steric repulsion. Here a sulfur atom comes on the top of a 1,3-dithiole ring, so that this is regarded as another kind of "ring-over-atom" interaction. This overlap mode may be called "twisted ring-over-atom mode".

The a1 interaction in δ-$(ET)_2AuBr_2$ is different from that of β-$(ET)_2AsF_6$ (Table 2). The former appears at $D = 0.3$ Å with almost the same ω. In Fig. 4, this position is located on the first ridge at $D = 0.0$ Å. Similarly to the AsF_6 salt, this is a staggered overlap as shown in Fig. 1(b), and is regarded as another type of twisted ring-over-atom mode. The $AuBr_2$-type overlap is also realized in δ-$(ET)_2AuI_2$. In Table 1, these two salts are listed separately. All other δ-phase salts, namely the majority of the δ-salts, have the usual AsF_6-type overlap.

Universal Phase Diagram. This type of structure has been observed in a considerable number of ET salts as listed in Table 1. The entries are aligned in the increasing order of the axis ratio c/a. There is a general tendency that T_{MI} decreases with increasing the axis ratio, though there are some irregularities. This is plotted in Fig. 5(a). From this figure, if we once know the axis ratio of a δ-phase, we can make a rough prediction of T_{MI}. This figure constructs the universal phase diagram of the δ-phase.

As c/a increases, the lattice expands along the c axis, and shrinks along the a axis. When a lattice constant shrinks, the intermolecular overlap integral increases, because the intermolecular distance decreases. Roughly speaking, the overlap integrals along a increase, and those along c decrease. The Fermi surface of the δ-phase is open with respect to the transverse (c) direction, Consequently, as c/a increases, the one-dimensionality decreases, or in other words the warping of the Fermi surface increases. Since the M–I transition is a Peierls transition,[6] this reduces T_{MI}. This is a naive explanation of the above phase diagram.

The halide salts, $(ET)_2Br(H_2O)_3$ and $(ET)_2Cl(H_2O)_3$ are the end members of Table 1, which have large c/a and comparatively low T_{MI}. The electrical resistivity of $(ET)_2Br(H_2O)_3$ shows a complicated behavior; the resistivity increases by several times below 150 K, but it becomes metallike again below 50 K.[10] This is reminiscent of the high-pressure resistivity of β-$(ET)_2PF_6$;[6] under the pressure above 5 kbar, the resistivity of β-$(ET)_2PF_6$ increases by several times at around $T_{MI} = 300$ K, whereas the resistivity remains almost constant down to about 50 K. These semimetallic behaviors are explained by imperfect nesting of the Fermi surface. Although the authors of Ref. 10 have reported a closed Fermi surface for $(ET)_2Br(H_2O)_3$, our re-examination has given an open Fermi surface that is basically the same as Fig. 2(b) (Table 3).

The metal cyanide salts δ-$(ET)_2M(CN)_4{\cdot}4H_2O$ [M = Ni and Pt] are located next to these halide salts, and have relatively low T_{MI}.[9] The Fermi surface that is basically the same as Fig. 2(b) has been reported for these compounds.[9] $(ET)_2Cl(H_2O)_2$ shows an exceptionally low $T_{MI} = 20$ K, which is consistent with its large c/a.[12] This phase has not been investigated in detail, probably because of the difficulty of its crystal growth.

In order to further explore the reason why the universal phase diagram holds in the δ-phase salts, overlap integrals of representative δ-phases are plotted in Fig. 5(b). The interactions c and p are comparatively insensitive to c/a. This is reasonable that the geometry parameters concerning to these interactions are approximately the same (Table 2). The a1 interaction also does not show any correlation to T_{MI}. By contrast, the q and a2 interactions change significantly. In particular, the interaction q shows a very good correlation to T_{MI}, as shown in Fig. 6. The q interaction reduces with the increase of T_{MI}. Since the magnitude of overlap integral may depend on the choice of semiempirical parameters used in the calculation, the geometry parameters of the q interaction are compared in Fig. 6. With the increase of T_{MI}, both the interplanar distance ΔZ and the displacement D increase. Both of these contribute to the reduction of the q interaction.

In the equation of the band dispersion (Eq. 1), the Δ term determines the warping, because only this term has k_a dependence. In the Δ term, the factors that are products of both $\cos k_c c$ and $\cos(k_a a/2)$ contribute to the imperfect nesting. For instance, if we focus on $2t_p \cos k_c c$ in the first parentheses, this term gives a contribution depending on $\cos k_c c \cos(k_a a/2)$. This term is proportional to the second parentheses, the square root of $t_{a2}^2 + t_q^2 + 2t_{a2}t_q \cos k_c c$. Since t_q is much larger than t_{a2} (Fig. 5(b)), t_q principally regulates the magnitude of this term, and consequently the warping of the Fermi surface. The first parentheses also contribute to the warping through the $2\ t_{a2}\ t_q \cos k_c c$ term in the second parentheses, whereas this term is again proportional to t_q, and the a1 and p interactions are comparatively insensitive to the axis ratio. From this perspective, the q interaction is the key interaction which regulates the magnitude of the

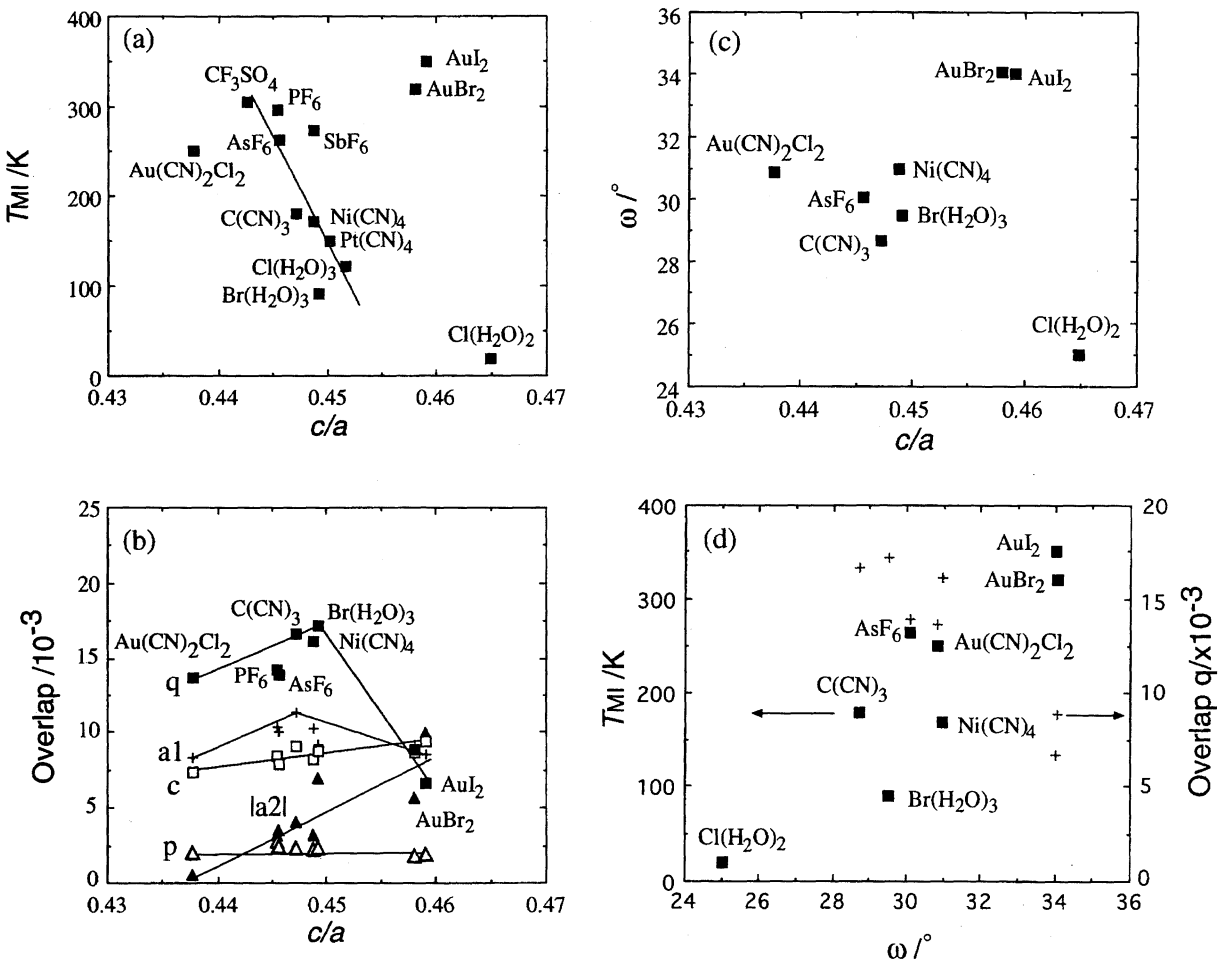

Fig. 5. (a) Metal-insulator transition temperatures of the δ-phase salts, plotted against the axis ratio. (b) Overlap integrals of the δ-phase salts, plotted against the axis ratio. (c) ω of the a1 interaction plotted against the axis ratio. (d) ω dependence of T_{MI} and the q interaction.

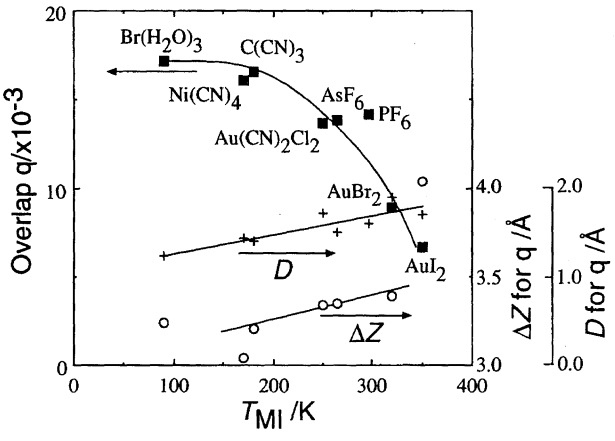

Fig. 6. Overlap integral q of the δ-phase salts, plotted against T_{MI}. Geometry parameters concerning to the q interaction, the displacement D along the molecular long axis, and the interplanar distance ΔZ are plotted together.

imperfect nesting. This does not contradict with the above naive explanation, where we have argued that an increase of *c/a* reduces the one-dimensionality.

In δ-$(ET)_2AuBr_2$ and δ-$(ET)_2AuI_2$, *c/a* seems to increase too much to maintain the same structure, and changes the overlap mode of a1. At the same time, the interstack interaction is modified, and particularly the q interaction is reduced considerably. As a result, T_{MI} rises significantly. These salts are plotted together in Fig. 6. It is remarkable that the same mechanism applies to these salts.

The energy band structure of δ-$(ET)_2AuBr_2$ has been reported in Ref. 13, and the results are essentially the same as those in Fig. 2(b). In this salt, two-fold lattice distortion along the transverse axis has been observed as well. However, Kobayashi et al.[14] and Whangbo et al.[15] have independently reported a closed Fermi surface for δ-$(ET)_2AuI_2$. Although Whangbo et al. have not reported the overlap integrals, their calculation seems to overestimate the overlaps along the stacking (*a*) axis. This affords a closed Fermi surface. On the contrary, our semiempirical parameters tend to give comparatively large transverse overlaps (Appendix in Part I). We have re-examined the Fermi surface of δ-$(ET)_2AuI_2$ by using the same semiempirical parameters, and have obtained an open Fermi surface that is basically the same as the other δ-phase salts. This agrees with the observed two-fold modulation of this compound.[15] Then we can conclude that the Fermi surfaces of these compounds are

essentially the same.

In Fig. 5(c), ω of the a1 interaction is plotted. The shapes of Figs. 5(a) and 5(c) are almost the same; ω shows a similar change to T_{MI}. Therefore, as shown in Fig. 5(d), with an increase of ω, the q interaction decreases, and T_{MI} increases. These relations hold including δ-$(ET)_2AuBr_2$ and δ-$(ET)_2AuI_2$. This reminds us of the θ-phase, where the dihedral angle is the key parameter which regulates T_{MI}. In the δ-phase, however, this is not directly through the a1 interaction, but indirectly through the q interaction.

In Table 1, some salts which have double conducting sheets, have $b = 34$ Å. In these salts, the inclination of the molecular long axis with respect to the conducting sheet takes alternately opposite directions in the succeeding conducting sheets. On the contrary, salts with a single sheet structure have $b = 17$ Å and here all inclinations are oriented in the same direction. Since this distinction does not alter the above rule, these two kinds of salts are listed together in Table 1.

δ'-Phase. Crystals of the usual δ-phase have orthorhombic or monoclinic symmetry; they have two-fold axes running along the crystallographic c axis (Fig. 3(a)). There is another modification where these two-fold axes are removed (Fig. 3(b)). This modification has triclinic symmetry, and has two crystallographically independent molecules in a unit cell. Since the distinction from the usual δ-phase has not been recognized seriously, there is no appropriate name for this low-symmetry δ-phase. We shall call this modification δ'-phase in the following discussion. The δ'-phase salts are listed in Table 1.

As one representative δ'-phase salt, crystal and energy band structures of $(ET)_2Br(C_2H_4(OH)_2)$ are depicted in Fig. 7. The overlap integrals and the geometry parameters of this salt are listed in Table 3. Owing to the breakdown of the symmetry, the a2, c, and q interactions are separated into two. In addition, half of the p interaction is lost as shown in Fig. 7(a). Furthermore, ϕ values of the a2 and a2′ interactions are about 90° (Table 3). Because D's of these interactions are about 1.4 Å, these are typical RB overlap modes. On the contrary, the a2 interaction in the usual δ-phase is an RA mode ($\phi = 60°$ and $D = 0.0$ Å) (Table 2). The change of the a1 overlap from the RB to the RA mode is the primary origin of the symmetry breakdown (Fig. 3).

The crystal distortion also alters the geometry of the q interaction; ϕ is reduced from 35° for the usual δ-phase to 22°. The latter direction is close to the point at which the overlap crosses zero (Fig. 2(a) in Part I), thus the q and q′ overlaps are comparatively small. Here the q overlap is again the key interaction which determines T_{MI}. This is the principal reason that the δ'-phase salts except for $(ET)_2Br(C_2H_4(OH)_2)$ are poor conductors (Table 1).

The displacement D of the a1 interaction, 1.9 Å is significantly shorter than the usual δ-phase (2.6 Å). As Fig. 4 shows, this is located near the trough of the overlap, so that the a1 overlap is rather small. In the δ'-phase, all transverse interactions, c, p, and q, as well as the interdimer interaction, a1 are small, whereas the intradimer overlaps a2 and a2′ are exceptionally large. Consequently the δ'-phase is regarded as a strongly dimerized structure with respect to the parallel a1 interaction, and the other interdimer interactions are weak. As shown in Fig. 7(b), the band structure has a one-dimensional character along the transverse (c) direction, but the bandwidth is relatively narrow. All these points are in agreement with the poor conductivity of the δ'-phase.

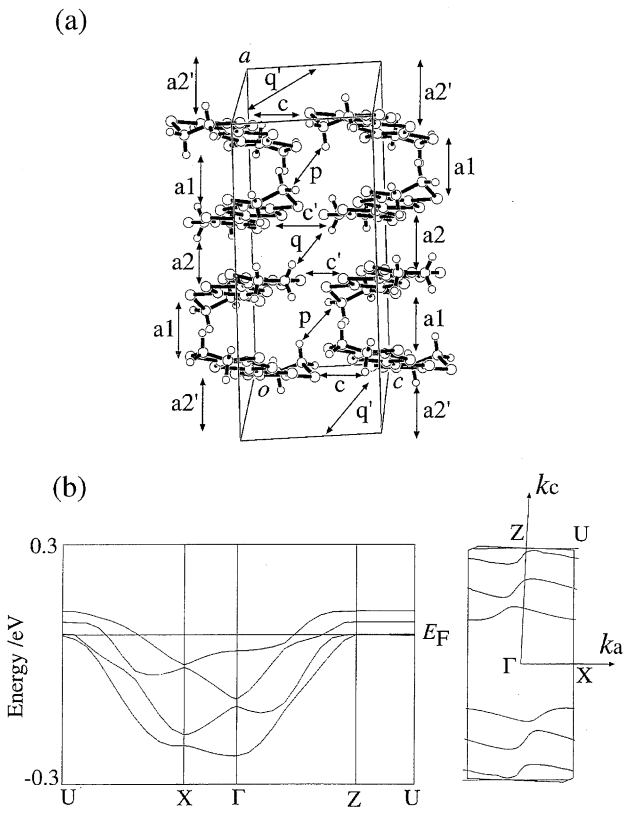

Fig. 7. (a) Structure of the donor sheet in δ'-$(ET)_2BrC_2H_4(OH)_2$, viewed approximately along the molecular long axis. (b) Energy band structure and Fermi surface of δ'-$(ET)_2BrC_2H_4(OH)_2$. The lattice is transformed so as to correspond with the δ-phase.

Table 3. Overlap Integrals ($\times 10^{-3}$) and Geometry Parameters in δ'-$(ET)_2Br(C_2H_4(OH)_2)$

Interaction	Overlap $\times 10^{-3}$	$X(D)$/Å	Y/Å	Z/Å	ϕ/°	ω/°
a1	3.0	1.9	(0.2)	(3.9)	(87)	31.7
a2	22.8	1.4	0.1	3.6	89	
a2′	24.7	1.3	0.0	3.6	90	
c	5.2	1.7	6.3	0.9	8	
c′	4.5	1.7	6.3	1.0	9	
p	3.0	3.6	(6.5)	(3.0)	(25)	
q	3.9	3.2	6.4	2.6	22	
q′	5.4	0.4	6.4	2.7	23	

$(ET)_2FeCl_4$ is a representative member of the δ'-phase. There are two different $(ET)_2FeCl_4$ salts with the same composition and different crystal structures; one has been reported by an English group,[18] and the other by a Chinese group.[21] The latter has four crystallographically independent molecules in a conducting sheet, but the former has only two,

similarly to the other δ'-phase salts. We cannot, however, discuss their structural differences further, because the structural detail of the latter has not been published. For a long time, another member $(ET)_2GaI_4$ has been recognized as a β-phase salt, because the authors of Ref. 20 have pointed out a similarity to β_{42}-$(ET)_2InBr_4$.[35] If we replace the twisted a1 interaction of the δ'-phase with a $\phi = 90°$ interaction with large dislocation ($D = 4.8$ Å in the case of $(ET)_2InBr_4$), a β_{42}-phase is constructed. In this sense, the δ'-phase is closely related to the β_{42}-phase.

α'-Phase. The above δ- and δ'-phases are composed of an alternate stack of twisted (a1) and parallel (a2) interactions. There is another group called α'-type, where all overlap modes in the stack are twisted (Fig. 8). In the stack, the molecules are twisted alternately in the opposite directions. In other words, the parallel layers of the δ-phase, which are composed of the a2 and q interactions, are removed. Here, only one molecule is crystallographically independent, and the molecules in the same stack are related by two-fold axes running along c, just like the δ-phase salts. Consequently, the α'-phase salts have a monoclinic symmetry. In the following discussion, the lattice constants of the α'-phase are transformed so as to coincide with those of the δ-phase (Table 1). It should be noticed that this phase has no structural relation either to the α-phase or to the α''-phase (Part II).

The overlap integrals and the geometry parameters of α'-$(ET)_2AuBr_2$ are listed in Table 4. The a1 interaction is the usual twisted overlap with $D = 2.4$ Å whereas the a2 interaction is the AuI_2-type overlap with $D = 0.2$ Å. The chain of the α'-phase consists of an alternate stack of these

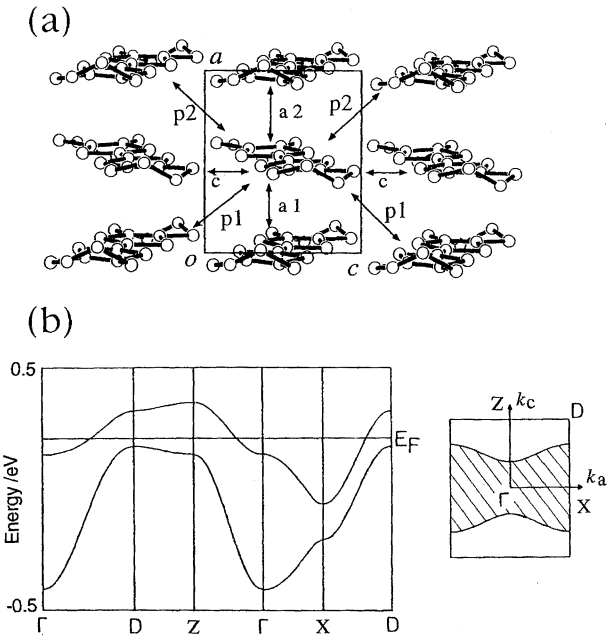

Fig. 8. (a) Structure of the donor sheet in α'-$(ET)_2AuBr_2$, viewed approximately along the molecular long axis. (b) Energy band structure and Fermi surface of α-$(ET)_2AuBr_2$. The lattice is transformed so as to correspond with the δ-phase.

Table 4. Overlap Integrals ($\times 10^{-3}$) and Geometry Parameters in α'-$(ET)_2AuBr_2$

Interaction	Overlap $\times 10^{-3}$	$X(D)$/Å	Y/Å	Z/Å	ϕ/°
a1	5.4	2.4	(0.7)	(3.5)	(79)
a2	11.9	0.2	(0.1)	(3.8)	(89)
c	8.7	1.9	6.5	0.0	13
p1	1.9	4.3	(5.8)	(3.5)	(31)
p2	1.9	1.7	(6.5)	(3.8)	(30)

two overlap modes.

The c interaction has a considerable magnitude, so that the Fermi surface is open with respect to the transverse (c) direction similarly to the δ-phase. This is in agreement with the observation of two-fold modulation along this direction. Naively speaking, the q interaction, which has been the key interaction to determine the magnitude of the warping in the δ-phase, is removed in the α'-phase. As a matter of fact, the p1 and p2 interactions contribute to distort the Fermi surface and to destroy the perfect nesting, but the magnitudes of these interactions are small. Hence, the good nesting accounts for the insulating properties of the α'-phase salts (Table 1).

The Fermi surface reported by Whangbo et al.[25] is open with respect to the stacking (a) direction, instead of the transverse (c) direction. Similarly to the calculation of δ-$(ET)_2AuI_2$,[15] this again seems to be due to an overestimation of the overlap integrals along the stacking direction. The observation of two-fold lattice modulation with the nesting vector (a, b, $2c$) in α'-$(ET)_2Ag(CN)_2$, α'-$(ET)_2Au(CN)_2$, and α'-$(ET)_2AuBr_2$,[25] is in good agreement with the present calculation (Fig. 8).

$(ET)_2N(CN)_2$ and $(ET)_2C_5(CN)_5(TCE)_x$ have basically the same structure, though the lattice along the stacking (a) axis is doubled (Table 1).[26,27] A repeating unit along this axis contains four molecules, whereas one molecule is crystallographically independent. These molecules are connected by two-fold axes running alternately along c and b axes. As a result, this phase has an orthorhombic symmetry.

γ'-$(ET)_2AuI_2$ is another modification of the α'-phase,[29] where all overlap modes in the stack are twisted overlap. The twisted molecules are, however, slid not along the molecular long axis (X), but along the molecular short (Y) axis. This is just like the situation when the RB overlap mode is replaced by the RA mode. The molecules in a stack are related by two-fold axes running along the b axis; this makes a sharp contrast with the α'-phase, where the two-fold axes are along the c axis. As a consequence, the molecular planes are tilted with respective to the stacking direction. A unit cell contains two columns along the c axis, and the molecules in these columns are tilted alternately in the opposite directions. The molecules belonging to different columns are related by two-fold axes running along the a axis. In this respect, this phase is related to the θ-phase, though the intrastack interaction is changed from the RA overlap to a twisted overlap. This is a very unique structure, which has no analogous salt.

The stack of $(ET)_3(HgCl_3)_2$ is made up of repetition of

two twisted overlaps ($\omega = 35°$, $D = 2.4$ Å) and one parallel overlap.[30] Then this phase is regarded as a 2:1 hybrid of the α'- and δ'-phases. The parallel overlap is a $\phi = 90°$ interaction, but D is very large (3.7 Å). From this, this phase should be taken as a "twisted trimer" structure.

Interestingly the twisted overlap mode has never been observed in BO and BETS salts.

Magnetic State in an Insulating Phase

In ET salts which undergo metal-insulator transitions, the magnetic property of the insulating phase is classified into two groups. Some salts show paramagnetic susceptibility, in which the susceptibility approximately follows the Bonner–Fisher-type temperature dependence. In this case there is usually no anomaly in the susceptibility at T_{MI}. Others become nonmagnetic in the insulating state; in these the susceptibility follows the singlet-triplet-type behavior below T_{MI}.

In the present series of papers, we have pointed out whether each compound becomes paramagnetic or nonmagnetic. One of the most puzzling example is the α'- and δ-phases, discussed in the former half of this paper. The α'-phase shows paramagnetic behavior and the δ-phase becomes nonmagnetic below T_{MI}.[6,36] Because both compounds have the one-dimensional Fermi surface with respect to the transverse direction, the only structural difference is two- or four-fold periodicity in the stacking direction. Obviously here is the key to resolve this puzzling problem.

One-Dimensional System. In order to account for the difference of the magnetic properties, first we shall investigate a one-dimensional system. We shall consider a dimerized chain illustrated in Fig. 9, where we assume that the energy band is one-quarter filled, and that a unit cell contains four molecules. Since the molecules form dimers, each spin is located on a dimer.

As far as all interdimer transfers are equivalent, as shown in Fig. 9(a), the system is paramagnetic. This situation may occur when the unit cell contains only two molecules, but we shall suppose that the equivalency of the transfers is attained by some symmetry operation, instead of the reduction of the lattice periodicity. When the interdimer transfers become alternately non-equivalent, as shown in Fig. 9(b), the system becomes nonmagnetic.

To translate this situation to crystallographer's language, we can say that in the paramagnetic phase (Fig. 9(a)), all molecules are crystallographically equivalent, so that all interdimer transfers are equivalent. To make all molecules equivalent, the existence of two kinds of symmetry operations is required. Usually the *interdimer* interaction itself is related by a symmetry operation, for instance, by an inversion center (Fig. 9(a)). If there is an additional symmetry operation which relates the *intradimer* interaction, for instance a two-fold axis, all molecules become equivalent and all interdimer transfers equivalent. Such symmetry properties are just the same as those of the stacking pattern of β-$(ET)_2AsF_6$ (Fig. 2(a) or Fig. 3(a)), although this compound is not one-dimensional in this direction.

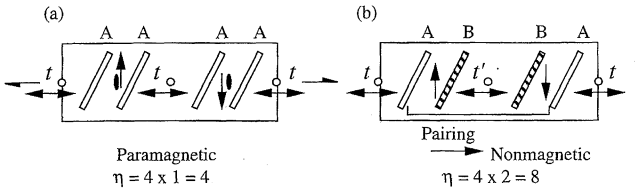

Fig. 9. One-dimensional quarter-filled chain with a dimerized structure. (a) Paramagnetic phase with equivalent interdimer transfers, and (b) nonmagnetic phase with nonequivalent transfers.

If we remove the two-fold axis, the two molecules of which the dimer is composed, become non-equivalent (A and B in Fig. 9(b)). In this case the two interdimer transfers becomes non-equivalent, because t is an interaction between A and A, and t' between B and B. This gives rise to pairing of the spins, where a spin gap proportional to $t^2 - t'^2$ is expected.

The pairing of the spins is decided by investigating whether the interdimer transfers are equivalent or not. The above discussion illustrates that *instead of the number of non-equivalent transfers, we may consider the number of non-equivalent molecules.*

If the transition from Fig. 9(a) to Fig. 9(b) is induced by temperature, this is a spin-Peierls transition. In the following, however, we shall discuss the symmetry of individual crystals. We shall also confine ourselves to the insulating phase just below T_{MI}, because an additional low-temperature transition such as a real spin-Peierls transition or an antiferromagnetic transition will remove the spin degree of freedom in any case.

Symmetry Number. In order to decide the existence of pair formation from crystal symmetry easily, we shall define "symmetry number" η as follows:

$$\begin{aligned}&\text{(Symmetr number) } \eta \\ &= \text{(Number of molecules in a unit cell)} \times \text{(Number of} \\ &\quad \text{crystallographically independent molecules).}\end{aligned} \tag{2}$$

In the case of Fig. 9, $\eta = 4\times1 = 4$ for (a), and $\eta = 4\times2 = 8$ for (b). The system is paramagnetic if η is less than or equal to four, and is nonmagnetic if η is larger than four. Although the symmetry number is an abstract concept, it represents the degree of symmetry; the larger η is, the lower the symmetry is. Every time η doubles, the symmetry reduces by one unit.

We can easily extend this criterion to two-dimensional cases. A two-dimensional system is composed of so many transfer integrals that it is not easy to decide whether the interdimer interactions are equivalent or not. However, systems of low symmetry with $\eta>4$ allows spin pair formation owing to the nonequivalent transfers, resulting in a nonmagnetic insulating state. On the contrary, high symmetry with $\eta\leq4$ gives rise to equivalent interdimer transfers and a paramagnetic insulating state. In Table 5 η is compared for representative ET salts in which the magnetic susceptibility has been reported. As shown in Table 5, the observations of susceptibility are in perfect agreement with this prediction.

Although this is an empirical rule that was originally ex-

Table 5. Symmetry Number η of ET Salts

Compound	Molecules in a cell		Independent molecules	η	Expected magnetism[a)]	Experiment[a)]	Ref.
$\beta_{21\times2}$-$(ET)_2ReO_4$	4		2	8	Non	Non	37
β'-$(ET)_2ICl_2$	2		1	2	Para	Para	38
β''_{411}-$(ET)_2Pd(CN)_4$	4		2	8	Non	Non	39
θ-$(ET)_2Cu_2(CN)[N(CN)_2]_2$	2		0.5	1	Para	Para	40
θ-$(ET)_2RbZn(SCN)_4$	2	$\times2$[b)]	0.5	2	Para	Para	41
α-$(ET)_2I_3$	4		2	8	Non	Non	42
α''-$(ET)_2Ag(CN)_2$	4		1	4	Para	Para	43
α''-$(ET)_2KCu(SCN)_4$	4		1	4	Para	Para	44
$\varkappa$-$(ET)_2Cu_2(CN)_3$	4		1	4	Para	Para	45
$\varkappa$-$(ET)_2Cu[N(CN)_2]Cl$	4		1	4	Para	Para	46
β-$(ET)_2PF_6$	4	$\times2$[b)]	1	8	Non	Non	6
α'-$(ET)_2AuBr_2$	2	$\times2$[b)]	1	4	Para	Para	36
$(ET)_2C_5(CN)_5(TCE)_x$	4		1	4	Para	Para	27

a) Non: Nonmagnetic, and Para: Paramagnetic. b) Two-fold superstructure.

tracted from the experimental results of magnetic susceptibility, this rule is based on pair formation when the spins are hypothetically located on the dimers, and universally applies to all ET salts. Before we discuss why this criterion holds, it is better to examine the individual crystals depicted in Fig. 10.[47]

Individual Crystals. In $\beta_{21\times2}$-$(ET)_2ReO_4$ (Fig. 10(a)), the upward and downward spins are placed on AB dimers, where open and shaded rectangles represent crystallographically independent molecules, A and B. These two dimers are connected by different transfers t and t', because t and t' are related by two different inversion centers. In two dimension there are many transfers between the two dimers, but the present argument examines, from the viewpoint of the symmetry, whether the interdimer interactions are equivalent or not as a whole. In this case, these upward and downward spins make a pair, and actually the system becomes nonmagnetic below $T_{MI} = 81$ K.[37]

β'-Phase contains only two molecules in a unit cell (Fig. 10(b)). Then one spin is placed in a unit cell, and obviously all spins are equivalent. This results in a paramagnetic insulating state.[38] The two molecules in a unit cell are connected by an inversion center, and only one molecule is crystallographically independent. It is instructive to imagine a crystal structure where this inversion center is removed, though such a crystal does not exist in reality. This leads to two independent molecules, and η becomes $2\times2 = 4$. Then, this system is still expected to be paramagnetic. In the real space, the pair of A and B molecules makes a dimer, but the interdimer interactions are equivalent, because the dimer still construct a unit cell. Consequently, all spins are equivalent, and a paramagnetic state results.

As shown in Fig. 10(c), β''_{411}-$(ET)_2Pd(CN)_4$ is in principle the same as $\beta_{21\times2}$-$(ET)_2ReO_4$. The spins are located on the hypothetical AB dimers. Since the interdimer transfers are non-equivalent, the system is expected to be nonmagnetic. Actually β''_{411}-$(ET)_2Pd(CN)_4$ becomes nonmagnetic below T_{MI}. In β''_{421}-$(ET)_2Pd(CN)_4{\cdot}H_2O$, however, the drop of ESR intensity is not obvious, partly due to the comparatively low T_{MI} (80 K).[39]

In θ-$(ET)_2Cu_2(CN)[N(CN)_2]_2$, half of a molecule is independent and a unit cell contains two molecules, so that η is one. This compound is insulating from room temperature, but remains paramagnetic down to low temperatures.[40] θ-$(ET)_2RbZn(SCN)_4$ has the same symmetry at high temperatures. Below $T_{MI} = 190$ K, η is doubled by the two-fold superstructure, but η is still two, resulting in no pairing. The observed susceptibility is Bonner–Fisher-like down to low temperatures.[41] In Fig. 10(d), the spins are located on arbitrary dimers (according to Hypothesis (2) in 47)), but these spins are not paired even if the cells are doubled.

It should be noted that, when the lattice is doubled on account of the occurrence of superstructure, we have multiplied η by two. Naively speaking, this seems reasonable because the volume of the lattice is doubled. From the structural point of view, however, lattice doubling is usually accompanied by the reduction of the crystal symmetry. When we attempt a structure analysis of the superstructure, the supercell has lower symmetry than the original cell at almost all times. If we then consider the symmetry of the supercell, η is more than two times larger than the original one. Table 5 tells us that we need not to take this into account, because we can correctly predict the magnetic properties of θ-$(ET)_2RbZn(SCN)_4$ ($\eta = 2$),[41] α'-$(ET)_2AuBr_2$ ($\eta = 4$),[36] and β-$(ET)_2PF_6$ ($\eta = 8$),[6] only by multiplying by two. This means that the number of the independent molecules are not effectively changed in the two-fold phase. When we consider a two-fold superstructure, we have to consider the *hidden symmetry*; the symmetry of the overlap integrals are, at least approximately, higher than the crystallographic requirements.

α-$(ET)_2I_3$ has a similar lattice to that of the doubled θ-phase (Fig. 10(e)), but the crystal symmetry is inherently low (belonging to the triclinic crystal system). When we place the spins on any dimers, the dimers are non-equivalent and the interdimer interactions are non-equivalent. The expected insulating state is nonmagnetic, and actually below $T_{MI} = 135$ K the susceptibility exhibits an activated behavior.[42]

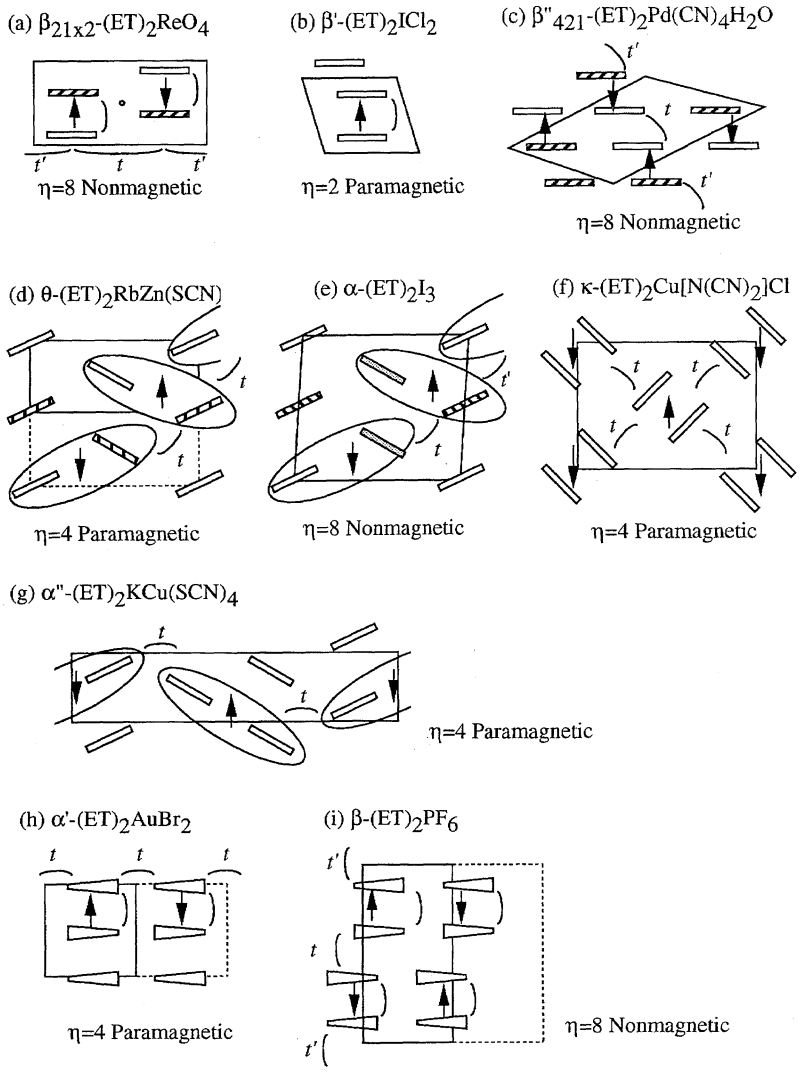

Fig. 10. Configuration of local spins when spins are located on hypothetical dimers. The shaded molecules represent the crystallographically independent molecules which should be distinguished from the unshaded molecules.

From the crystal symmetry,[48] α-$(ET)_2KHg(SCN)_4$ has $\eta = 8$ and is potentially nonmagnetic as well as α-$(ET)_2I_3$. The distortion from the θ-phase is, however, very small in the former compound. Furthermore, in the experiments of quantum oscillations under high magnetic fields, magnetic breakdown has been reported.[49] When $\eta \leq 4$, the Fermi surface is expected to be a large connected one like the θ-phase. By contrast, when $\eta > 4$, there appears a gap between the open and closed parts of the Fermi surface. The observation of the magnetic breakdown indicates that this gap is very small. Therefore the symmetry is very close to that of the $\eta = 4$ state. Unfortunately the quantum chemical calculation tends to overestimate this kind of gap, because the slightly distorted structure gives rise to an enhanced distortion of the orbitals, which in turn results in a large difference in the overlap integrals. If α-$(ET)_2KHg(SCN)_4$ has a hidden $\eta = 4$ symmetry, this accounts for the nature of the 8 K anomaly, which is most likely a spin-density-wave state.

The $\varkappa$-phase has a definite dimer structure, and we can place spins on the dimers (Fig. 10(f)). Since the interdimer p and q interactions are equivalent for all cases, there is no pairing of the dimers, and the system remains paramagnetic ($\eta = 4$). This is exemplified by the insulating phase of $\varkappa$-$(ET)_2Cu_2(CN)_3$,[45] and the low-temperature insulating state of $\varkappa$-$(ET)_2Cu[N(CN)_2]Cl$.[46]

The $\varkappa$-phase is, however, located on a marginal position. Some $\varkappa$-salts are non-centrosymmetric mainly due to the reduced symmetry of the anions, so that the two molecules composing the dimer are crystallographically independent. This results in $\eta = 8$, and if the distortion is large enough, insulating states of non-centrosymmetric $\varkappa$-phases are potentially nonmagnetic. However, representative non-centrosymmetric $\varkappa$-phases such as $\varkappa$-$(ET)_2Cu(NCS)_2$,[50] $\varkappa$-$(ET)_2Cu(CN)[N(CN)_2]_2$,[51] and $\varkappa$-$(ET)_2Ag(CN)_2 \cdot H_2O$,[52] are metals down to low temperatures. Among a series of $\varkappa$-salts with the compositions $\varkappa$-$(ET)_2Hg(SCN)_2X$ [X = Cl, Br, and I] and $\varkappa$-$(ET)_2Hg(SCN)Cl_2$,[53—55] two salts containing chlorine atoms ($\varkappa$-$(ET)_2Hg(SCN)_2Cl$ and $\varkappa$-$(ET)_2Hg(SCN)Cl_2$) are non-centrosymmetric, and two other Br and I salts are centrosymmetric. ESR intensity of all these compounds decrease more or less below T_{MI}.[55,56] Further study is, however, necessary to confirm these results. It is sometimes difficult

only from the observation of ESR intensity to decide whether an insulating phase is paramagnetic or nonmagnetic. In particular, when T_{MI} is low (<100 K), the drop of susceptibility is obscured by the presence of the Curie tail.

Among the compounds that have distorted $\varkappa$-like structures, $(ET)_4PtCl_4PhCN$ has a distorted triclinic lattice, so that η is 8.[57] This salt undergoes a M–I transition at 250 K, below which the susceptibility falls down to zero, in agreement with the expected nonmagnetic state. $(ET)_4(Et_4N)M(CN)_6\cdot 3H_2O$ [M = Fe and Co] also has a triclinic lattice with $\eta = 8$.[58] Although these compounds are reported to be semiconductors at room temperature, there is a sharp drop of susceptibility at around 230 K for the Co salt. The existence of magnetic ions, however, complicates the magnetic properties of these compounds.

Another marginal case is α''-phase. The symmetry number is 4, and paramagnetism is predicted (Fig. 10(g)).[44] In α''-$(ET)_2CsHg(SCN)_4$,[59] however, two-fold superlattice reflections similar to those of θ-$(ET)_2RbZn(SCN)_4$ have been observed even above T_{MI}.[60] The two-fold supercell leads to $\eta = 8$, and a nonmagnetic state. Actual α''-phases show paramagnetic susceptibility, but the susceptibility deviates from the Bonner–Fisher behavior and decreases more rapidly at low temperatures; the temperature dependence has been fitted by the alternating Heisenberg model, where the spin gap originating from the dimerization is in the order of 20 K. In this case, the development of the two-fold modulation around 250 K is accompanied by about a 20% drop of the magnetic susceptibility. These observations are explained if we assume that the two-fold lattice modulation generates a small spin gap, whose magnitude is in the order of 20 K. Like this, the distinction between paramagnetic and nonmagnetic is not obvious in some cases, and the magnitude of the spin gap must be discussed quantitatively.

As shown in Fig. 10(h), α'-$(ET)_2AuBr_2$ has $\eta = 4$ by taking the two-fold supercell into account, and paramagnetism is predicted. By contrast, β-$(ET)_2PF_6$ leads to $\eta = 8$ and a nonmagnetic insulating state (Fig. 10(i)). These predictions completely agree with the experiments.[6,36] In the former half of this paper, we have discussed the nesting of the α'-phase, as if the insulating phase was the Peierls state. This is not true, because the insulating phase is a paramagnetic Mott–Hubbard insulator, which has a charge gap but does not have a spin gap. In this context, we have to treat the charge excitation and the spin excitation independently, and consider the "nesting" of the susceptibility concerning the charge excitation.

Summary. In summary, magnetic properties are predicted by investigating the symmetry of the hypothetical states where each spin is localized onto each dimer. *If the upward and downward spins make a pair in view of the crystal symmetry, the insulating state is nonmagnetic, and otherwise it is paramagnetic.*

This leads to the following simple rule that determines the magnetic state in a quarter-filled band:

(1) Phases that contain two molecules in a unit cell (β, β', β'', and θ) are paramagnetic at all times.

(2) Phases that contain four molecules in a unit cell are divided to two cases:

(a) Salts with a triclinic lattice have two nonequivalent molecules, giving rise to pairing and a nonmagnetic insulating state. Examples are $\beta_{21\times2}$-$(ET)_2ReO_4$ and β_{411}-$(ET)_2Pd(CN)_4$.

(b) Salts with a higher than monoclinic lattice have two-fold axes (α') or two-fold screw axes (α'', and $\varkappa$), which make all molecules equivalent, leading to a paramagnetic insulating state.

Other Band Filling. We can extend this discussion to general band filling other than the quarter-filled band. If the energy band is 1/n-filled, the critical η is expected to be n. For example, β''_{311}-$(ET)_3(ClO_4)_2$ has 1/3-filled band, so that $\eta_c = 3$. This compound contains three molecules in a unit cell, and one and a half molecules are crystallographically independent (Fig. 11). Here a molecule located on an inversion center is regarded as a half unit. Then η is $3\times1.5 = 4.5$, and a nonmagnetic state is expected. This compound show singlet-triplet-type susceptibility below T_{MI} = 170 K.[61] α-$(ET)_3(ReO_4)_2$ ($\eta = 4.5$, this is a kind of β''-phase as well) is also reported to show an activated susceptibility below T_{MI} = 88 K.[37]

$\beta''_{321\times2}$-$(ET)_3Cl_2(H_2O)_2$ involves six molecules in a unit cell and three of them are crystallographically independent.[62] Hence η is $6\times3 = 18$, and a nonmagnetic state is predicted. The static magnetic susceptibility of this compound exhibits a clear drop below T_{MI} = 100 K.[63]

Site-Equivalency. In a half-filled case, the critical symmetry number is $\eta_c = 2$. As shown in Fig. 12(a), when a unit cell contains only one molecule, η is $1\times0.5 = 0.5$, and a paramagnetic state is predicted correctly. However, if a unit cell contains two molecules (Fig. 12(b)), the transfer integrals are alternately different, and obviously the system is nonmagnetic. The symmetry number is $\eta = 2\times1 = 2$, which is equal to η_c, and a paramagnetic state is expected incorrectly. As shown in Fig. 12(c), there is another configuration, where a unit cell contains two molecules. Here two molecules are located on inversion centers, and half of each is crystallographically independent. This structure results in the same $\eta = 2\times(2\times0.5) = 2$, but is paramagnetic because all transfers are equivalent. In this case, the symmetry number rule works correctly.

To distinguish Figs. 12(b) and 12(c), these structures will be designated as "site-equivalent" and "site-nonequivalent", respectively. In a half-filled system, the symmetry number

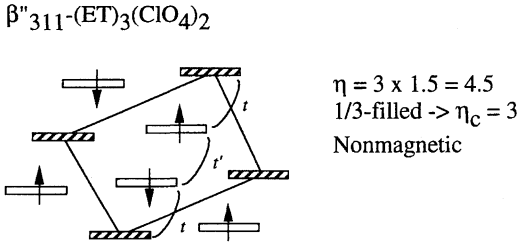

Fig. 11. Configuration of local spins in a one-third filled system, β''_{311}-$(ET)_3(ClO_4)_2$.

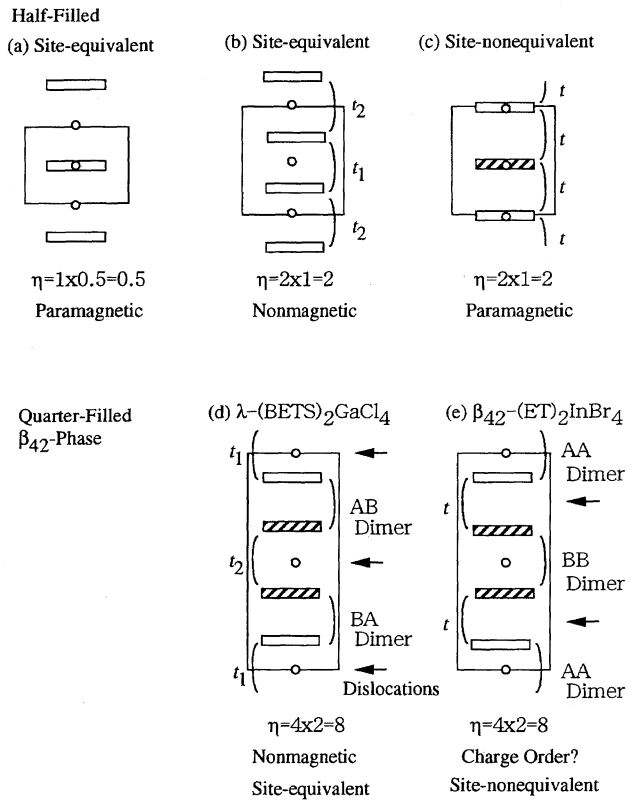

Fig. 12. Half filled systems with (a) one molecule in a unit cell, (b) two equivalent molecules, and (c) two nonequivalent molecules in a unit cell. Quarter-filled β_{42}-phases; (d) equivalent dimers in λ-$(BETS)_2GaCl_4$, and (e) nonequivalent dimers in β_{42}-$(ET)_2InBr_4$.

rule holds for site non-equivalent configurations. In the preceding discussion, we have implicitly assumed the site-equivalent configuration, as stated in working hypothesis (3). In a half-filled system, paramagnetic or nonmagnetic is easily decided by investigating whether the transfers are equivalent or not. To avoid confusion, it is better *not to apply the symmetry number rule to a half-filled system.*

It is noteworthy to consider the site-nonequivalent configuration in an ordinary quarter-filled system. For instance, site-equivalent and site-nonequivalent patterns for β_{42}-structure are depicted in Figs. 12(d) and 12(e). The site-equivalent structure (Fig. 12(d)) has dislocations (indicated by arrows) on inversion centers, so that AB molecules form a dimer. As a result, the interdimer transfers t_1 and t_2 are nonequivalent, because t_1 is located between A and A molecules, and t_2 is between B and B. This structure is realized in superconducting λ-$(BETS)_2GaCl_4$.

In the site-nonequivalent structure in Fig. 12(e), the dislocation is present between A and B, so that AA pair and BB pair form two kinds of dimers. This makes two nonequivalent dimers, but all interdimer transfers t become equivalent, because they connect A and B molecules. This structure is realized in β_{42}-$(ET)_2InBr_4$. Recently Tanaka et al. have found this structure in λ'-$(BETS)_2GaBr_4$, and designated this structure as λ'-phase.[64]

In general, in a given couple of site-equivalent and site-nonequivalent patterns with the same symmetry number, the product of the number of the sites and the number of nonequivalent transfers is constant, so that, if the number of the nonequivalent sites (or dimers) increases, the number of the transfers decreases.

Charge Order. It has sometimes been observed that charge is not evenly distributed on molecules. For the sake of simplicity, we shall first consider an entirely charge ordered state as A^0B^+. For instance, in the β_{42}-structure in Fig. 12(d), we shall imagine a state in which all charge is located on the shaded molecules. As far as we may neglect the existence of the neutral A^0 molecules and only consider the B^+ molecules instead of the $(AB)^+$ dimers, the equivalency of the "interdimer" transfers is not altered, so that a nonmagnetic state is expected. Accordingly the prediction of the symmetry number rule does not change even under the charge ordered state. This is valid even under fractional charge distribution.

However, experimentally, charge-ordered states are usually paramagnetic. This is not surprising because a charge-ordered state has a well-established local spin on A^+. The insulating state is not associated with the Peierls-like singlet pair formation, as assumed in the nonmagnetic insulators. On the contrary, the uneven distribution and the resulting localization of the charge is the origin of the insulating state. It is needless to say that many charge-ordered states have another transition to a spin singlet state or an antiferromagnetic state at low temperatures. In some compounds, if an insulating state is paramagnetic in spite of the large η (>4), we have a good reason to suspect the occurrence of charge order.

Examples of Charge Order. To be fair, examples that seem to break the symmetry number rule should be noticed. An ET salt that involves a large polyanion, $(ET)_8[SiW_{12}O_{40}]$, contains eight molecules in a unit cell, and two of them are crystallographically independent.[65] Then η is $8\times2=16$. Since this salt is formally quarter-filled, a nonmagnetic state is expected. This compound is insulating at room temperature, but exhibits the Heisenberg-like susceptibility down to low temperatures, in contradiction with the symmetry number rule.[66] The structure is, however, composed of θ-like array of two kinds of columns, I and II, and charge separation like I^+II^0 has been reported. The column I is made up of a perfectly uniform stack, so that it is reasonable that a uniform half-filled band gives rise to the paramagnetic susceptibility.

Another possible example is δ'-phase. As shown in Fig. 7, a δ'-phase contains four molecules and two independent molecules, so that η is $4\times2=8$, suggesting a nonmagnetic state. Susceptibility of δ'-$(ET)_2BrC_2H_4(OH)_2$ shows a sharp drop of about 50% at T_{MI} = 196 K, but decreases very gradually down to 80 K, below which the susceptibility decays exponentially.[67] The state between 196 and 80 K seems to be paramagnetic, in conflict with the symmetry number rule. Moreover, δ'-$(ET)_2GaCl_4$ is insulating even at room temperature, but exhibits Bonner–Fisher-like susceptibility.[16] However, there is a spin gap of the order of 50 K.[68] Otherwise, these observations suggest the possibility of the charge sep-

aration in these δ'-phase salts.

In this context, the symmetry number rule is a *necessary* condition that makes the system nonmagnetic, but not a sufficient condition. In a few examples discussed above, the prospective nonmagnetic systems have exhibited paramagnetism. There are no opposite exceptions, where a prospective paramagnetic system becomes nonmagnetic. The symmetry number rule may break when: (1) The difference of t and t' is *accidentally* so small that the resulting spin gap is smaller than k_BT_{MI}. (2) The insulator phase is made up of irregular spin pair formation which leaves some unpaired spins. Alternatively inhomogeneous charge distribution may result in unpaired spins as well. These exceptions are, fortunately, not many. The important point is that the singlet states in two-dimensional organic conductors are associated with the "crystal fields" or with the difference of t and t'.[69]

Superconductivity. Although we have discussed the insulating states, we can define η for metallic compounds. We shall designate the metals with $\eta>4$ as "potentially nonmagnetic" metals, and others as "potentially paramagnetic" metals. For example, such salts as β-$(ET)_2I_3$, β''-$(ET)_2AuBr_2$, $\varkappa$-$(ET)_2Cu[N(CN)_2]Br$, and θ-$(ET)_2I_3$ are potentially paramagnetic metals. On the other hand, α-$(ET)_2NH_4Hg(SCN)_4$, $(ET)_4H_2O[Fe(ox)_3]PhCN$, and λ-$(BETS)_2GaCl_4$ are potentially nonmagnetic metals.

By extending this argument, we can divide superconductors to potentially paramagnetic and nonmagnetic ones. Table 6 lists these classifications.

There is a remarkable common feature in the potentially nonmagnetic superconductors. All superconductors have 2×2 or 42 subscripts. In the former, two dimers are aligned in the transverse direction in a unit cell, as shown in Fig. 10(a), and the latter has two dimers stacked in the columnar direction (Fig. 12(d)). These structures are "dimerized dimer" structures. Tetramer phases such as β''_{412}-$(ET)_2ClO_4(TCE)_{0.5}$ and β''_{411}-$(ET)_2Pt(CN)_4$ do not exhibit superconductivity. It is particularly remarkable that β''_{412}-$(ET)_2ClO_4(TCE)_{0.5}$ is not superconducting even though it is metallic down to low temperatures.

Table 6. Classifications of Superconductors

ET-Based	Other donors
Potentially paramagnetic	
β-Phase	$(TMTSF)_2X$
$\varkappa$-Phase	$(DMET)_2X$
	$(DTEDT)_3Au(CN)_2$
Potentially nonmagnetic	
$\beta_{21\times2}$-$(ET)_2ReO_4$	$\beta''_{20\times2}$-$(BO)_2ReO_4\cdot H_2O$
$\beta''_{211\times2}$-$(ET)_2SF_5CF_2SO_3$	
β''_{421}-$(ET)_2Pt(CN)_4\cdot H_2O$	
β''_{421}-$(ET)_2Pd(CN)_4\cdot H_2O$	
$\beta''_{321\times2}$-$(ET)_3Cl_2(H_2O)_2$	
β''_{431}-$(ET)_4H_2O[Fe(ox)_3]PhCN$	
α-$(ET)_2NH_4Hg(SCN)_4$	
θ-$(ET)_2I_3$	

TMTSF: tetramethyltetraselenafulvalene. DMET: dimethyl(ethylenedithio)diselenadithiafulvalene. DTEDT: 2-(1,3-dithil-2-ylidene)-5-(2-ethanediylidene-1,3-dithiole)-1,3,4,6-tetrathiapentalene. BO: bis(ethylendioxy)tetrathiafulvalene.

In the three-quarter filled salts, the superconductors have double column structures such as $\beta''_{321\times2}$-$(ET)_3Cl_2(H_2O)_2$ and β''_{431}-$(ET)_4H_2O[Fe(ox)_3]PhCN$. Dimerized dimer structure is also realized in these superconductors.

Salts that have dimerized dimer structure, but do not show superconductivity, are very few. $\beta_{21\times2}$-$(ET)_2BrO_4$ is isostructural to superconducting $\beta_{21\times2}$-$(ET)_2ReO_4$, but T_{MI} is very high (150 K). β''_{421}-$(ET)_2Ni(CN)_4\cdot H_2O$ also has too high T_{MI} = 180 K. β_{42}-$(ET)_2InBr_4$ possibly suffers from charge ordering owing to the site-nonequivalent structure. Therefore there are good reasons that these salts do not show superconductivity.

Among the representative potentially paramagnetic phases, β''_{211}-$(ET)_2AuBr_2$ and β'-$(ET)_2X$ are not superconductors. To eliminate these phases, the existence of large connected two-dimensional Fermi surface is regarded as the necessary condition of superconductivity. A dimer structure is also common to these superconducting phases. This rule, however, only applies to ET-based superconductors. In case of selenium-containing donors, like TMTSF and DMET, the salts with open Fermi surface also show superconductivity. This is the same for DTEDT, which has large π-framework. The magnitude of the on-site Coulomb repulsion U is important in this respect.

We can therefore summarize the requirement of superconductivity:

(1) Potentially paramagnetic salts: Dimer structure and large-connected two-dimensional Fermi surface for ET-based superconductors. Moderate warping in open Fermi surface is sufficient for selenium-containing donors.

(2) Potentially nonmagnetic salts: Dimerized dimer structure.

It has been believed that the prediction of superconductivity is very difficult. From the above criteria, however, we can make fairly good predictions about superconductivity. It has been particularly mysterious for a long time that, in addition to the β- and $\varkappa$-phase superconductors with high symmetry, there are several low-symmetry superconductors. The present discussion demonstrates that these superconductors can be classified in the potentially nonmagnetic group, and there are definite rules for these superconductors. It should be pointed out that the above rules are only the necessary conditions for superconductivity. β-$(ET)_2I_2Br$ does not show superconductivity owing to the anion disorder. Not all $\varkappa$-phase salts show superconductivity (Part II). There may be an additional requirement such as the balance of U and the bandwidth, but this is judged from the universal phase diagram, as discussed in Part II.

Two superconductors, α-$(ET)_2NH_4Hg(SCN)_4$ and θ-$(ET)_2I_3$, do not clearly fall into either of the above categories. However, the former has a weakly dimerized dimer structure, in a broad sense. If the periodicity of the anion is taken into account in the latter salt, this is also the same situation.

It is beyond the scope of the present work to provide the sufficient theoretical background for the above criteria. Superconductivity mediated by site-local attraction has been recently investigated extensively.[70] For instance, in the dimerized dimer structure in Fig. 10(a), the spin configuration depicted in the figure, where one up-spin and one down-spin occupy each dimer in the cell, forming a pair, is more stable than any other configurations. This may give rise to the attractive force between the electrons located on the neighboring dimers, and promotes the singlet spin pair formation. Although this driving force is the same as that making the spin gap, if the electrons are mobile enough, this may contribute to the formation of the Cooper pairs.

The potentially paramagnetic superconductors have dimer structures as well, so that they have effectively half-filled two-dimensional bands. In this respect, they have a close resemblance to the copper oxides. In these compounds, spin fluctuation gives rise to nearest neighbor attraction, which may be the origin of the Cooper pair formation. In the copper oxides, the antiferromagnetic instability is suppressed by doping, and is replaced by superconductivity. In the $\varkappa$- and β-phases, however, the exactly half-filled band together with the triangular lattice seems to be important for superconductivity.

These considerations suggest somewhat different mechanisms of superconductivity in the potentially nonmagnetic and paramagnetic organic superconductors. From the above discussion, the potentially nonmagnetic superconductors prefer singlet pair formation, though it is not necessarily s-wave. On the other hand, the potentially paramagnetic superconductors have many common points with the copper oxides, in which d-wave pairing has been established.[71] Furthermore, when the superconducting phases border on insulating phases, the potentially nonmagnetic superconducting phase is located near a spin-singlet insulating phase, whereas the potentially paramagnetic phase borders on a paramagnetic insulator phase. As a most naive model, in the g-ology in one dimension, a singlet superconducting phase borders on a CDW phase, and a triplet superconducting phase neighbors on an SDW phase.[72] A similar phase diagram has been proposed for two dimensional square lattices, where the triplet phase is replaced by a d-wave phase.[71] Investigations of pair anisotropy in organic conductors have been undertaken only for the potentially paramagnetic superconductors, though, even in that case, the conclusions have not entirely converged.

In summary we have investigated the classifications of phases with twisted molecules. The δ-phase consists of the twisted dimer and the RA overlap, and the δ'-phase is composed of the twisted dimer and the RB overlap, whereas the α'-phase is made up only of the twisted overlaps. Since the twisted overlap is not very sensitive to the geometry, the change of ω, and indirectly the axis ratio, regulate the warping of the Fermi surface and consequently T_{MI}, through the change of the q interaction; this is the key interaction in the δ-phase.

The symmetry number rule of the magnetic state of insulating phases has been proposed. By counting the number of molecules in a unit cell, and the number of crystallographically independent molecules, we can make a good prediction whether the insulating phase will be paramagnetic or nonmagnetic. This is based on the possibility of pair formation of the spins, from the viewpoint of the crystal symmetry.

This distinction is able to be extended to superconductors. If we once classify superconductors into potentially paramagnetic and potentially nonmagnetic ones, we can extract a common structural feature of superconductors, and we can determine the necessary conditions for superconductivity.

The author is grateful to Dr. G. K. R. Senadeera for help of the energy band calculations.

References

1 T. Mori, *Bull. Chem. Soc. Jpn.*, **71**, 2509 (1998).
2 H. Kobayashi, T. Mori, R. Kato, A. Kobayashi, Y. Sasaki, G. Saito, and H. Inokuchi, *Chem. Lett.*, **1983**, 581.
3 U. Geiser, B. A. Anderson, A. Murray, C. M. Pipan, C. A. Rohl, B. A. Vogt, H. H. Wang, and J. M. Williams, *Mol. Cryst. Liq. Cryst.*, **181**, 105 (1990).
4 D. Chasseau, D. Watkin, M. J. Rosseinsky, M. Kurmoo, D. R. Talham, and P. Day, *Synth. Met.*, **24**, 117 (1988).
5 R. Laversanne, J. Amiell, P. Delhaes, D. Chasseau, and C. Hauw, *Solid State Commun.*, **52**, 177 (1984).
6 G. K. R. Senadeera, T. Kawamoto, T. Mori, J. Yamaura, and T. Enoki, *J. Phys. Soc. Jpn.*, **67**, 4193 (1998).
7 M. A. Beno, H. H. Wang, L. Soderholm, K. D. Carlson, L. N. Hall, L. Nunez, H. Rummens, B. Anderson, J. A. Schueter, J. M. Williams, M.-H. Whangbo, and M. Evain, *Inorg. Chem.*, **28**, 150 (1989).
8 H. Yamochi, T. Tsuji, G. Saito, T. Suzuki, T. Miyashi, and C. Kabuto, *Synth. Met.*, **27**, A479 (1988).
9 M. Fettouhi, L. Ouahab, D. Grandjean, L. Ducasse, J. Amiell, R. Canet, and P. Delhaes, *Chem. Mater.*, **7**, 461 (1995).
10 M. Luo, T. Ishida, A. Kobayashi, and T. Nogami, *Synth. Met.*, **96**, 97 (1998); Q. Zhang, P. Wu, Y. Li, and D. Zhu, *Synth. Met.*, **98**, 129 (1998).
11 G. Bravic, D. Chasseau, J. Gautier, M. J. Rosseinsky, M. Kurmoo, P. Day, and A. Filhol, *Synth. Met.*, **42**, 2035 (1991).
12 R. P. Shibaeva, R. M. Lobkovskaya, L. P. Rozenberg, L. I. Buravov, A. A. Ignatiev, N. D. Kushch, E. E. Laukhina, M. K. Makova, E. B. Yagubskii, and A. V. Zvarukina, *Synth. Met.*, **27**, A189 (1988).
13 T. Mori, F. Sakai, G. Sito, and H. Inokuchi, *Chem. Lett.*, **1986**, 1589.
14 A. Kobayashi, R. Kato, H. Kobayashi, M. Tokumoto, H. Anzai, and T. Ishiguro, *Chem. Lett.*, **1986**, 1117.
15 M.-H. Whangbo, M. Evain, M. A. Beno, H. H. Wang, K. S. Webb, and J. M. Williams, *Solid State Commun.*, **68**, 421 (1988).
16 M. Kurmoo, M. Allan, R. H. Friend, D. Chasseau, G. Bravic, and P. Day, *Synth. Met.*, **42**, 2127 (1991).
17 U. Geiser, H. H. Wang, S. Kleinjan, and J. M. Williams, *Mol. Cryst. Liq. Cryst.*, **181**, 125 (1990).
18 T. Mallah, C. Hollis, S. Bott, M. Kurmoo, P. Day, M. Allan, and R. H. Friend, *J. Chem. Soc., Dalton Trans.*, **1990**, 859.
19 N. P. Karpova, S. V. Konovalikhin, O. A. Dyachenko, R. N. Lyubovskaya, and E. I. Zhilyaeva, *Acta Crystallogr., Sect. C*, **C48**, 62 (1992).

20 U. Geiser, H. H. Wang, J. A. Schlueter, S. L. Hallenbeck, T. J. Allen, M. Y. Chen, H.-C. I. Kao, K. D. Carlson, L. E. Gerdom, and J. M. Williams, *Acta Crystallogr., Sect. C*, **C44**, 1544 (1988).

21 H. Yu, B. Zhang, and D. Zhu, *J. Mater. Chem.*, **8**, 77 (1998).

22 X. Bu, I. Cisarova, and P. Coppens, *Acta Crystallogr., Sect. C*, **C48**, 1563 (1992).

23 H. Kobayashi, R. Kato, T. Mori, A. Kobayashi, Y. Sasaki, G. Saito, T. Enoki, and H. Inokuchi, *Chem. Lett.*, **1984**, 179.

24 M. Kurmoo, D. R. Talham, P. Day, J. A. K. Howard, A. M. Stringer, D. S. Obertelli, and R. H. Friend, *Synth. Met.*, **22**, 415 (1988).

25 M. A. Beno, M. A. Firestone, P. C. W. Leung, L. M. Sowa, H. H. Wang, J. M. Williams, and M.-H. Whangbo, *Solid State Commun.*, **57**, 735 (1986).

26 X. Bu and P. Coppens, *Acta Crystallogr., Sect. C*, **C48**, 1560 (1992).

27 W. H. Watson, A. M. Kini, M. A. Beno, L. K. Montgomery, H. H. Wang, K. D. Carlson, B. D. Gates, S. F. Tytko, J. Derose, C. Crariss, C. A. Rohl, and J. M. Williams, *Synth. Met.*, **33**, 1 (1989).

28 S. Sekizaki, H. Yamochi, and G. Saito, private communication.

29 U. Geiser, H. H. Wang, M. A. Beno, M. A. Firestone, K. S. Webb, J. M. Williams, and M.-H. Whangbo, *Solid State Commun.*, **57**, 741 (1986).

30 R. P. Shibaeva, L. P. Rozenberg, M. Z. Aldoshina, and R. N. Lyubovskaya, *Sov. Phys. Crystallogr.*, **33**, 71 (1988).

31 T. Mori, H. Mori, and S. Tanaka, *Bull. Chem. Soc. Jpn.*, **72**, 179 (1999).

32 P. C. W. Leung, M. A. Beno, G. S. Blackman, B. R. Coughlin, C. A. Miderski, W. Joss, G. W. Crabtree, and J. M. Williams, *Acta Crystallogr., Sect. C*, **C40**, 1331 (1984).

33 T. Mori, A. Kobayashi, Y. Sasaki, R. Kato, and H. Kobayashi, *Solid State Commun.*, **53**, 627 (1985).

34 R. Laversanne, J. Amiell, P. Delhaes, D. Chasseau, and C. Hauw, *Mol. Cryst. Liq. Cryst.*, **120**, 405 (1985).

35 M. A. Beno, D. D. Cox, J. M. Williams, and J. F. Kwak, *Acta Crystallogr., Sect. C*, **C40**, 1334 (1984).

36 S. D. Obertelli, R. H. Friend, D. R. Talham, M. Kurmoo, and P. Day, *J. Phys. Condens. Matter.*, **1**, 5671 (1989).

37 K. Carneiro, J. C. Scott, and E. M. Engler, *Solid State Commun.*, **50**, 477 (1984).

38 N. Yoneyama, A. Miyazaki, T. Enoki, and G. Saito, *Synth. Met.*, **86**, 2029 (1997).

39 T. Mori, K. Kato, Y. Maruyama, H. Inokuchi, H. Mori, I. Hirabayashi, and S. Tanaka, *Synth. Met.*, **56**, 2911 (1992).

40 T. Komatsu, H. Sato, T. Nakamura, M. Matsukawa, H. Yamochi, G. Saito, M. Kusunoki, K. Sakaguchi, and S. Kagoshima, *Bull. Chem. Soc. Jpn.*, **68**, 2233 (1995).

41 H. Mori, S. Tanaka, and T. Mori, *Phys. Rev. B*, **57**, 12023 (1998).

42 B. Rothaemel, L. Forro, J. R. Cooper, J. S. Schilling, M. Weger, P. Bele, H. Brunner, D. Schweizer, and H. J. Keller, *Phys. Rev. B*, **34**, 704 (1986).

43 M. Kurmoo, P. Day, T. Mitani, H. Kitagawa, H. Shimoda, D. Yoshida, P. Guionneau, Y. Barrans, D. Chasseau, and L. Ducasse, *Bull. Chem. Soc. Jpn.*, **69**, 1233 (1996).

44 H. Mori, T. Okano, N. Sakurai, S. Tanaka, K. Kajita, and H. Moriyama, *Chem. Lett.*, **1998**, 505.

45 T. Komatsu, N. Matsukawa, T. Inoue, and G. Saito, *J. Phys. Soc. Jpn.*, **65**, 1340 (1996).

46 K. Miyagawa, A. Kawamoto, Y. Nakazawa, and K. Kanoda, *Phys. Rev. Lett.*, **75**, 1174 (1995).

47 To illustrate this figure, we have assumed the following working hypotheses:
(1) Placing spins is an entirely artificial process which we can carry out without the knowledge of amplitudes of the actual transfer integrals.
(2) When molecules are equivalent, any choice of dimer leads to the same result.
(3) When there are non equivalent molecules, choose a pair of non equivalent molecules as a dimer. This makes all dimers equivalent, and makes the interdimer interaction as much as non equivalent. This point will be discussed in the context of charge separation. It should be emphasized that we are investigating the symmetry of the crystal, but not discussing the actual position of the localized electrons.

48 H. Mori, S. Tanaka, M. Oshima, G. Saito, T. Mori, Y. Maruyama, and H. Inokuchi, *Bull. Chem. Soc. Jpn.*, **63**, 2183 (1990).

49 S. Uji, T. Terashima, H. Aoki, J. S. Brooks, M. Tokumoto, N. Kinoshita, T. Kinoshita, Y. Tanaka, and H. Anzai, *Phys. Rev. B*, **54**, 9332 (1996); M. M. Honold, N. Harrison, M.-S. Nam, J. Singlton, C. H. Mielke, M. Kurmoo, and P. Day, *Phys. Rev. B*, **58**, 7560 (1998).

50 H. Urayama, H. Yamochi, G. Saito, S. Sato, A. Kawamoto, J. Tanaka, T. Mori, Y. Maruyama, and H. Inokuchi, *Chem. Lett.*, **1988**, 463.

51 T. Komatsu, T. Nakamura, N. Matsukawa, H. Yamochi, G. Saito, H. Ito, T. Ishiguro, M. Kusunoki, and K. Sakaguchi, *Solid State Commun.*, **80**, 843 (1991); **82**, 101 (1992).

52 H. Mori, I. Hirabayashi, S. Tanaka, T. Mori, and H. Inokuchi, *Solid State Commun.*, **76**, 35 (1990).

53 M. Z. Aldoshina, R. N. Lyubovskaya, S. V. Konovalikhin, O. A. Dyachenko, G. V. Shilov, M. K. Makova, and R. B. Lyubovskii, *Synth. Met.*, **56**, 1905 (1993).

54 E. I. Yudanova, L. M. Makarova, S. V. Konovalikhin, O. A. Dyachenko, R. B. Lyubovskii, and R. N. Lyubovskaya, *Synth. Met.*, **79**, 201 (1996).

55 E. I. Yudanova, S. K. Hoffmann, A. Graja, S. V. Konovalikhin, O. A. Dyachenko, R. B. Lubovskii, and R. N. Lyubovskaya, *Synth. Met.*, **73**, 227 (1995).

56 E. I. Yodanova, R. N. Lyubovskaya, R. B. Lyubovskii, S. V. Konovalikhin, and O. A. Dyachenko, *Synth. Met.*, **86**, 2195 (1997).

57 A. A. Galimzyanov, A. A. Ignat'ev, N. D. Kushch, V. N. Laukhin, M. K. Makova, V. A. Merzhanov, L. P. Rozenberg, R. P. Shivaeva, and E. B. Yagubskii, *Synth. Met.*, **33**, 81 (1989).

58 P. L. Magueres, L. Ouahab, N. Conan, C. J. Gomez-Garcia, P. Delhaes, J. Even, and M. Bertault, *Solid State Commun.*, **97**, 27 (1996).

59 H. Mori, S. Tanaka, T. Mori, Y. Maruyama, H. Inokuchi, and G. Saito, *Solid State Commun.*, **78**, 49 (1991).

60 S. Hanazato, T. Mori, H. Mori, and S. Tanaka, *Physica C*, **316**, 243 (1999).

61 M. Kobayashi, T. Enoki, K. Imaeda, H. Inokuchi, and G. Saito, *Phys. Rev. B*, **36**, 1457 (1987).

62 T. Mori and H. Inokuchi, *Chem. Lett.*, **1987**, 1657; M. J. Rosseinsky, M. Kurmoo, D. R. Talham, P. Day, D. Chasseau, and D. Watkin, *J. Chem. Soc., Chem. Commun.*, **1988**, 88; T. Mori and H. Inokuchi, *Solid State Commun.*, **82**, 525 (1987).

63 S. D. Obertelli, I. R. Marsden, R. H. Friend, M. Kurmoo, M. J. Rosseinsky, P. Day, F. L. Pratt, and W. Hayes, in "Physics and Chemistry of Organic Superconductors," ed by G. Saito and S. Kagoshima, Splinger, Berlin (1990), p. 181.

64 H. Tanaka, A. Kobayashi, and H. Kobayashi, *Chem. Lett.*,

1999, 133.

65 A. Davidson, K. Boubekeur, A. Penicaud, P. Auban, C. Lenoir, P. Batail, and G. Herve, *J. Chem. Soc., Chem. Commun.*, **1989**, 1373.

66 C. Bellito, M. Bonamico, and G. Staulo, *Mol. Cryst. Liq. Cryst.*, **232**, 155 (1993).

67 A. Miyazaki, K. Yamaguchi, T. Enoki, and G. Saito, *Synth. Met.*, **86**, 2033 (1997).

68 N. Yoneyama, A. Miyazaki, T. Enoki, and G. Saito, *Bull. Chem. Soc. Jpn.*, **72**, 4 (1999).

69 H. Kino and H. Fukuyama, *J. Phys. Soc. Jpn.*, **64**, 1877 (1995).

70 For a review, see: R. Micnas, J. Ranninger, and S. Robaszkiewicz, *Rev. Mod. Phys.*, **62**, 113 (1990).

71 D. J. Scalapino, *Phys. Rep.*, **250**, 329 (1995).

72 J. Solyom, *Adv. Phys.*, **28**, 201 (1979).